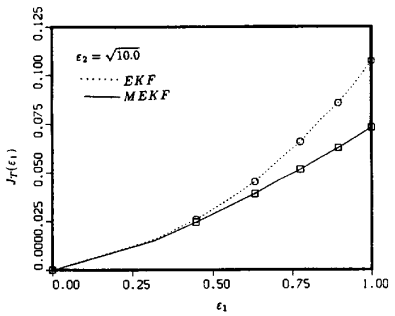

Fig. 9. Integral squared error $J_T(\epsilon_1)$.

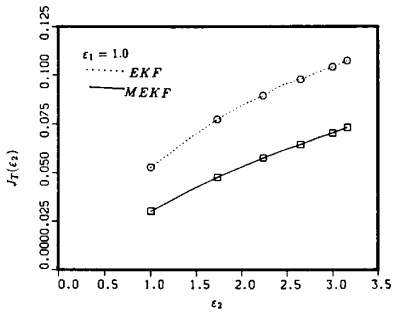

Fig. 10. Integral squared error $J_T(\epsilon_2)$.

References

[1] H. J. Kushner, "Dynamical equations for optimal nonlinear filtering," *J. Diff. Equations*, vol. 3, pp. 179–190, 1967.

[2] R. S. Bucy, "Nonlinear filtering theory,"*IEEE Trans. Automat. Contr.*, vol. 10, pp. 198–212, 1965.

[3] R. S. Liptser and A. N. Shiryayev, *Studies of Random Processes I and II.* Berlin: Springer-Verlag, 1978.

[4] M. Zakai, "On the optimal filtering of diffusion processes," *Z. Wahrsch., Verw. Geb.*, vol. 11, pp. 230–243, 1969.

[5] N. U. Ahmed, *Elements of Finite Dimensional Systems and Control Theory.* New York: Wiley and Sons,

[6] N. U. Ahmed, and T. E. Dabbous, "Nonlinear filtering of systems governed by Ito differential equations with jump parameters," *J. Math Anal. Appl.*, vol. 115, no. 1, pp. 76–92, 1986.

[7] A. H. Jazwinski, *Stochastic Processes and Filtering Theory.* New York: Academic, 1970.

Coordinating Locomotion and Manipulation of a Mobile Manipulator

Yoshio Yamamoto and Xiaoping Yun

***Abstract*—A mobile manipulator in this study is a manipulator mounted on a mobile platform. Assuming the end point of the manipulator is guided, e.g., by a human operator to follow an arbitrary trajectory, it is desirable that the mobile platform is able to move as to position the manipulator in certain preferred configurations. Since the motion of the manipulator is unknown *a priori*, the platform has to use the measured joint position information of the manipulator for its own motion planning. This paper presents a control algorithm for the platform so that the manipulator is always positioned at the preferred configurations measured by its manipulability. Simulation results are presented to illustrate the efficacy of the algorithm. The algorithm is also implemented and verified on a real mobile manipulator system. The use of the resulting algorithm in a number of applications is also discussed.**

I. Introduction

When a person writes across a board, he positions his arm in a comfortable writing configuration by moving his body rather than reaching out his arm. Also, when people transport a large and/or heavy object cooperatively, they prefer certain configurations depending on various factors, e.g., the shape and the weight of the object, the transportation velocity, the number of people involved in a task, and so on. Therefore, when a mobile manipulator performs a manipulation task, it is desirable to bring the manipulator into certain preferred configurations by appropriately planning the motion of the mobile platform. If the trajectory of the manipulator end point in a fixed coordinate system (world coordinate system) is known *a priori*, then the motion of the mobile platform can be planned accordingly. If the motion of the manipulator end point is unknown *a priori*, e.g., driven by a visual sensor or guided by a human operator, the path planning has to be made locally and in real time rather than globally and off line. This paper presents a control algorithm for the platform in the latter case, which takes the measured joint displacement of the manipulator as the input for motion planning and controls the platform to bring the manipulator into a preferred operating region. While this region can be selected based on any meaningful criterion, the manipulability measure [1] is utilized in this study. By using this algorithm, the mobile platform will be able to "understand the intention of its manipulator and respond accordingly." Since the mobile platform is subject to nonholonomic constraints, the control algorithm is developed using nonholonomic system theory.

This control algorithm has a number of immediate applications. First, a human operator can easily move around the mobile manipulator by "dragging" the end point of the manipulator while the manipulator is in the free mode (compensating the gravity only). Second, if the manipulator is force-controlled, the mobile manipulator

Manuscript received March 5, 1992; revised March 29, 1993 and June 28, 1993. This work was supported in part by NSF Grants BCS-92-16691, CISE/CDA-90-2253, IRI-92-09880, CDA-92-22732, and CISE/CDA 88-22719; ONR/DARPA Grants N0014-92-J-1647 and N0014-88-K-0630; Army/DAAL Grant 03-89-C-0031PRI; the Whitaker Foundation; and the University of Pennsylvania Research Foundation.

The authors are with the General Robotics and Active Sensory Perception (GRASP) Laboratory, University of Pennsylvania, Philadelphia, PA 19104-6228 USA.

IEEE Log Number 9401658.

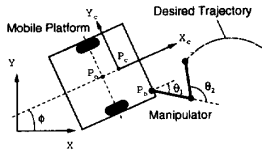

Fig. 1. Schematic of the mobile manipulator.

will be able to push against and follow an external moving surface. Third, when two mobile manipulators transport a large object with one being the master and the other being the slave, this algorithm can be used to control the slave mobile manipulator to support the object and follow the motion of the master, resulting in a cooperative control algorithm for two mobile manipulators.

Although there has been a vast amount of research effort on mobile platforms (commonly referred to as mobile robots) in the literature, studies on mobile manipulators are very limited. Joshi and Desrochers [2] considered a two-link manipulator on a moving platform subject to random disturbances in its orientation. Wien [3] studied dynamic coupling between a planar vehicle and a one-link manipulator on the vehicle. Liu and Lewis [4] proposed a decentralized robust controller for a wheeled mobile manipulator which considered the base and the manipulator as two separate subsystems. Dubowsky, Gu, and Deck [5] derived the dynamic equations of a spatial mobile manipulator with link flexibility. Recently, Hootsmans [6] proposed a mobile manipulator control algorithm (the Mobile Manipulator Jacobian Transpose Algorithm) for a dynamically coupled mobile manipulator. He showed that with the algorithm, the manipulator could successfully compensate the trajectory error caused by vehicle's passive suspension with the help of limited sensory information from mobile vehicle.

What makes the coordination problem of locomotion and manipulation a difficult one is twofold. First, a manipulator and a mobile platform, in general, have different dynamic characteristics, namely, a mobile platform has a slower dynamic response than a manipulator. Second, a wheeled mobile platform is subject to nonholonomic constraints while a manipulator is usually unconstrained. These two issues must be taken into consideration in developing control algorithms.

Dynamic modeling of mechanical systems with nonholonomic constraints is richly documented by work ranging from Neimark and Fufaev's comprehensive book [7] to more recent developments (see for example, [8]). The literature on control properties of such systems, however, is sparse [9], [10]. The interest in control of nonholonomic systems has been stimulated by the recent research in robotics. The dynamics of a wheeled mobile robot is nonholonomic [11] and so is a multi-arm system manipulating an object through the whole arm manipulation [12].

Bloch and McClamroch [9] first demonstrated that a nonholonomic system cannot be feedback stabilized to a single equilibrium point by a smooth feedback. In a follow-up paper [13], they showed that the system is small-time locally controllable. Campion *et al.* [14] showed that the system is controllable regardless of the structure of nonholonomic constraints provided that the constraints are independent and there is at least one control for each degree of freedom (DOF) of unconstrained motion. Yamamoto and Yun [15] proved that a nonholonomic system is not input-state linearizable. Because of these negative results on feedback stabilization and linearization, the control problem of nonholonomic systems is more difficult. Motion planning of mobile robots has been an active topic in robotics in the past several years [11], [16]–[19]. Nevertheless, much less is known about the dynamic control of mobile robots with nonholonomic constraints and the developments in this area are very recent [20]–[22].

In this paper, we first derive the constraint and motion equations of the mobile platform. We then present a feedback control algorithm developed for the mobile platform for coordinating locomotion and manipulation of the mobile manipulator. Finally we present the simulation and experimental results.

II. Modeling of the Mobile Platform

A. Constraint Equations

In this subsection, we derive the constraint equations for a LABMATE®[1] mobile platform. The platform has two driving wheels (the center ones) and four passive supporting wheels (the corner ones). The two driving wheels are independently driven by two dc motors. The following notations will be used in the derivation of the constraint equations and dynamic equations (see Fig. 1).

- P_o: the intersection of the axis of symmetry with the driving wheel axis;
- P_c: the center of mass of the platform;
- P_b: the location of the manipulator on the platform;
- P_r: the reference point to be followed by the mobile platform;
- d: the distance from P_o to P_c;
- b: the distance between the driving wheels and the axis of symmetry;
- r: the radius of each driving wheel;
- m_c: the mass of the platform without the driving wheels and the rotors of the dc motors;
- m_w: the mass of each driving wheel plus the rotor of its motor;
- I_c: the moment of inertia of the platform without the driving wheels and the rotors of the motors about a vertical axis through P_o;
- I_w: the moment of inertia of each wheel and the motor rotor about the wheel axis;
- I_m: the moment of inertia of each wheel and the motor rotor about the wheel diameter.

There are three constraints. The first one is that the platform must move in the direction of the axis of symmetry, i.e.,

$$\dot{y}_c \cos\phi - \dot{x}_c \sin\phi - d\dot{\phi} = 0 \tag{1}$$

where (x_c, y_c) are the coordinates of the center of mass P_c in the world coordinate system, and ϕ is the heading angle of the platform measured from the X axis of the world coordinates. The other two constraints are the rolling constraints, i.e., the driving wheels do not slip,

$$\dot{x}_c \cos\phi + \dot{y}_c \sin\phi + b\dot{\phi} = r\dot{\theta}_r \tag{2}$$

$$\dot{x}_c \cos\phi + \dot{y}_c \sin\phi - b\dot{\phi} = r\dot{\theta}_l \tag{3}$$

where θ_r and θ_l are the angular displacement of the right and left wheels, respectively.

Letting $q = (x_c, y_c, \phi, \theta_r, \theta_l)$, the three constraints can be written in the form of

$$A(q)\dot{q} = 0 \tag{4}$$

[1] LABMATE® is a trademark of Transitions Research Corporation.

where

$$A(q) = \begin{bmatrix} -\sin\phi & \cos\phi & -d & 0 & 0 \\ -\cos\phi & -\sin\phi & -b & r & 0 \\ -\cos\phi & -\sin\phi & b & 0 & r \end{bmatrix}. \quad (5)$$

It can be shown that among the three constraints, two of them are nonholonomic and the other one is holonomic [15]. In principle, one can always eliminate variables using holonomic constraints when deriving dynamic equations. Nevertheless, the elimination may be cumbersome in practice. To show the generality of the control method which is able to incorporate both holonomic and nonholonomic constraints, we treat both kinds of constraints in the same way; that is, we do not eliminate variables by using holonomic constraints.

B. Dynamic Equations

We now derive the dynamic equations for the mobile platform. The Lagrange equations of motion of the platform with the Lagrange multipliers λ_1, λ_2, and λ_3 are given by

$$m\ddot{x}_c - m_c d(\ddot{\phi}\sin\phi + \dot{\phi}^2\cos\phi) - \lambda_1\sin\phi - (\lambda_2+\lambda_3)\cos\phi = 0 \quad (6)$$

$$m\ddot{y}_c + m_c d(\ddot{\phi}\cos\phi - \dot{\phi}^2\sin\phi) + \lambda_1\cos\phi - (\lambda_2+\lambda_3)\sin\phi = 0 \quad (7)$$

$$-m_c d(\ddot{x}_c\sin\phi - \ddot{y}_c\cos\phi) + I\ddot{\phi} - d\lambda_1 + b(\lambda_3-\lambda_2) = 0 \quad (8)$$

$$I_w\ddot{\theta}_r + \lambda_2 r = \tau_r \quad (9)$$

$$I_w\ddot{\theta}_l + \lambda_3 r = \tau_l \quad (10)$$

where

$$m = m_c + 2m_w$$
$$I = I_c + 2m_w(d^2+b^2) + 2I_m$$

and τ_r and τ_l are the torques acting on the wheel axis generated by the right and left motors, respectively. These five equations of motion can be written in the vector form as

$$M(q)\ddot{q} + V(q,\dot{q}) = E(q)\tau - A^T(q)\lambda. \quad (11)$$

In the equation above, the matrix $A(q)$ has been defined in (5), and the matrices $M(q)$, $V(q,\dot{q})$, and $E(q)$ are given by

$$M(q) = \begin{bmatrix} m & 0 & -m_c d\sin\phi & 0 & 0 \\ 0 & m & m_c d\cos\phi & 0 & 0 \\ -m_c d\sin\phi & m_c d\cos\phi & I & 0 & 0 \\ 0 & 0 & 0 & I_w & 0 \\ 0 & 0 & 0 & 0 & I_w \end{bmatrix}$$

$$V(q,\dot{q}) = \begin{bmatrix} -m_c d\dot{\phi}^2\cos\phi \\ -m_c d\dot{\phi}^2\sin\phi \\ 0 \\ 0 \\ 0 \end{bmatrix}, \qquad E(q) = \begin{bmatrix} 0 & 0 \\ 0 & 0 \\ 0 & 0 \\ 1 & 0 \\ 0 & 1 \end{bmatrix}.$$

Next, we will represent the motion equation (11) and the constraint equation (4) in state space by properly choosing a state vector. To do so, we define a 5×2-dimensional matrix $S(q)$ such that $A(q)S(q) = 0$. It is straightforward to verify that the following matrix has the required property

$$S(q) = [s_1(q),\ s_2(q)] = \begin{bmatrix} c(b\cos\phi - d\sin\phi) & c(b\cos\phi + d\sin\phi) \\ c(b\sin\phi + d\cos\phi) & c(b\sin\phi - d\cos\phi) \\ c & -c \\ 1 & 0 \\ 0 & 1 \end{bmatrix}$$

where the constant $c = (r/2b)$. From the constraint equation (4), $\dot{q}$ is in the null space of $A(q)$. Because the two columns of $S(q)$ are in the null space of $A(q)$ and are linearly independent, it is possible to express $\dot{q}$ as a linear combination of the two columns of $S(q)$, that is,

$$\dot{q} = S(q)\nu. \quad (12)$$

The rationale behind (12) is to introduce a set of independent velocity variables, ν. Owing to the choice of $S(q)$ matrix, we have

$$\nu = \begin{bmatrix} \nu_1 \\ \nu_2 \end{bmatrix} = \begin{bmatrix} \dot{\theta}_r \\ \dot{\theta}_l \end{bmatrix}.$$

Differentiating equation (12), substituting the expression for $\ddot{q}$ into (11), and premultiplying it by S^T, we have

$$S^T(MS\dot{\nu}(t) + M\dot{S}\nu(t) + V) = \tau. \quad (13)$$

Using the state-space vector $x = [q^T\ \nu^T]^T = [x_c\ y_c\ \phi\ \theta_r\ \theta_l\ \dot{\theta}_r\ \dot{\theta}_l]^T$, we will be able to represent the constraint and motion equations of the mobile platform in state space.

$$\dot{x} = \begin{bmatrix} S\nu \\ f_2 \end{bmatrix} + \begin{bmatrix} 0 \\ (S^TMS)^{-1} \end{bmatrix}\tau \quad (14)$$

where $f_2 = (S^TMS)^{-1}(-S^TM\dot{S}\nu - S^TV)$. This state equation can be further simplified to

$$\dot{x} = \begin{bmatrix} S\nu \\ 0 \end{bmatrix} + \begin{bmatrix} 0 \\ I \end{bmatrix}u \quad (15)$$

by applying the following nonlinear feedback

$$\tau = S^TMS(u - f_2). \quad (16)$$

III. Control Algorithm

A. Output Equation

While the state equation of a dynamic system is uniquely, modulo its representation, determined by its dynamic characteristics, the output equation is chosen in such a way that the tasks to be performed by the dynamic system can be conveniently specified and that the controller design can be easily accomplished. For example, if a six-DOF robot manipulator is to perform pick-and-place or trajectory tracking tasks, the six-dimensional joint position vector or the six-dimensional Cartesian position and orientation vector is normally chosen as the output equation. In this subsection, we present the output equation for the mobile platform and discuss its properties.

It is convenient to define a platform coordinate frame $X_c - Y_c$ at the center of mass of the mobile platform, with X_c in the forward direction of the platform. We may choose a point P_r with respect to the platform coordinate frame $X_c - Y_c$ as a reference point. The mobile platform is to be controlled so that the reference point follows a desired trajectory. Let the reference point be denoted by (x_r^c, y_r^c) in the platform frame $X_c - Y_c$. Then the world coordinates (x_r, y_r) of the reference point are given by

$$x_r = x_c + x_r^c\cos\phi - y_r^c\sin\phi \quad (17)$$

$$y_r = y_c + x_r^c\sin\phi + y_r^c\cos\phi. \quad (18)$$

The selection of the reference point for the purpose of coordinating locomotion and manipulation is discussed in the following subsection. Having chosen the reference point, x_r^c and y_r^c are constant. By taking the coordinates of the reference point to be the output equation

$$y = h(q) = [x_r\quad y_r]^T \quad (19)$$

we have a trajectory tracking problem studied in [20], [21].

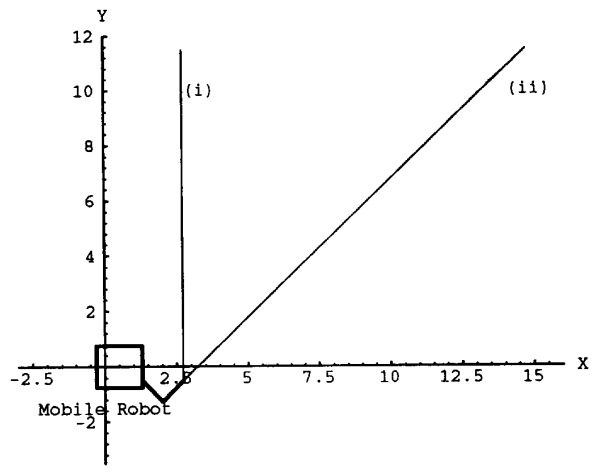

Fig. 2. Two desired trajectories for the simulation.

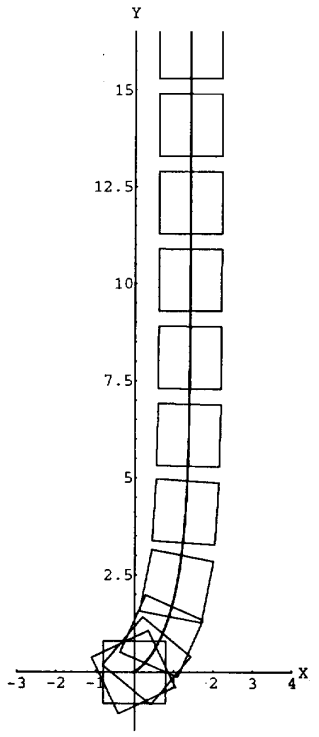

Fig. 3. Trajectory of the point P_o for Case i).

B. Feedback Control

Since the state equation (15) is not input-state linearizable [15], we will pursue input–output linearization with the output equation (19). The necessary and sufficient condition for input–output linearization is that the decoupling matrix has full rank [23]. The decoupling matrix for this output is

$$\Phi(q) = J_h(q)S(q) = \begin{bmatrix} \Phi_{11} & \Phi_{12} \\ \Phi_{21} & \Phi_{22} \end{bmatrix} \tag{20}$$

where

$$\Phi_{11} = c((b - y_r^c)\cos\phi - (d + x_r^c)\sin\phi)$$

$$\Phi_{12} = c((b + y_r^c)\cos\phi + (d + x_r^c)\sin\phi)$$

$$\Phi_{21} = c((b - y_r^c)\sin\phi + (d + x_r^c)\cos\phi)$$

$$\Phi_{22} = c((b + y_r^c)\sin\phi - (d + x_r^c)\cos\phi).$$

Since the determinant of the decoupling matrix is $\det(\Phi(q)) = -(r^2(d + x_r^c)/2b)$, it is singular if and only if $x_r^c = -d$, that is, the point P_r is located on the wheel axis. Therefore, trajectory tracking of a point on the wheel axis including P_o is not possible as pointed out in [21]. This is clearly due to the presence of nonholonomic constraints. A point on the wheel axis instantaneously has only one degree of freedom whereas any other point instantaneously has two degrees of freedom. Choosing x_r^c not equal to $-d$, we may decouple and linearize the system.

The nonlinear feedback for achieving input–output linearization is given by [23]

$$u = \Phi^{-1}(q)(v - \dot{\Phi}(q)\nu). \tag{21}$$

The linearized and decoupled subsystems are

$$\ddot{y}_1 = v_1 \tag{22}$$

$$\ddot{y}_2 = v_2. \tag{23}$$

A linear feedback is further designed for each subsystem to obtain the specified performance requirements. As described in the next subsection, the end point of the manipulator when it is at the preferred configuration is set as the reference point. By choosing the actual trajectory of the manipulator end point as the desired trajectory of the reference point (output equation), the reference point tracks the motion of the end point resulted from the human operator's drag. Consequently, the manipulator is maintained at the preferred configuration. We note that the actual trajectory of the end point is computed from the joint encoder measurements by using the manipulator direct kinematics.

C. Preferred Manipulator Configuration

While the human operator drags the end point of the manipulator, the mobile platform is controlled to bring the manipulator into a preferred configuration. Here we describe the preferred configuration chosen in this study. For simplicity, a two-link planar manipulator is considered in this discussion. Let θ_1 and θ_2 be the joint angles and L_1 and L_2 be the link length of the manipulator. Also let the coordinates of the manipulator base with respect to the platform frame $X_c - Y_c$ be denoted by (x_b^c, y_b^c). We set the reference point to the end point of the manipulator at a preferred configuration. We choose as the preferred configuration the one that maximizes the manipulability measure of the manipulator. If we specify the position of the end point as the desired trajectory for the reference point, the mobile platform will move in such a way that the manipulator is brought into the preferred configuration.

The manipulability measure can be regarded as a distance measure of the manipulator configuration from singular ones at which the manipulability measure becomes zero. At or near a singular configuration, the end point of the manipulator may not easily move in certain directions. The effort of maximizing the manipulability measure leads to keeping the manipulator configuration away from singularity. This notion is very important especially when a mobile manipulator is

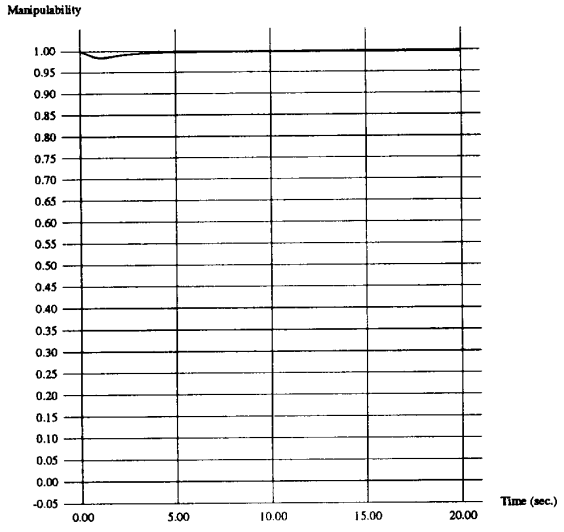

Fig. 4. Manipulability measure for Case i).

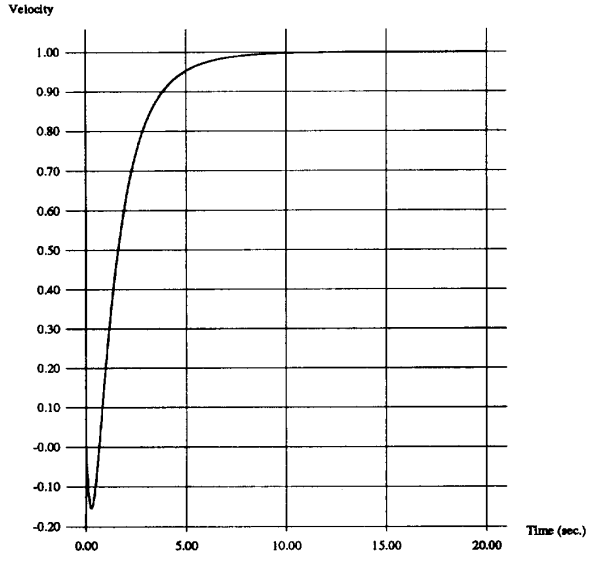

Fig. 5. Velocity of the point P_o for Case i).

required to respond to motions whose range is unknown *a priori*. The manipulability measure is defined as [1]

$$w = \sqrt{\det\left(J(\theta)J^T(\theta)\right)} \tag{24}$$

where θ and $J(\theta)$ denote the joint vector and Jacobian matrix of the manipulator. If we consider nonredundant manipulators, (24) reduces to

$$w = |\det J(\theta)|. \tag{25}$$

For the two-link manipulator shown in Fig. 1, the manipulability measure w is

$$w = \mid \det J \mid = L_1 L_2 \mid \sin\theta_2 \mid . \tag{26}$$

Note that the manipulability measure is maximized for $\theta_2 = \pm 90^\circ$ and arbitrary θ_1. We choose $\theta_2 = +90^\circ$ and $\theta_1 = -45^\circ$ to be

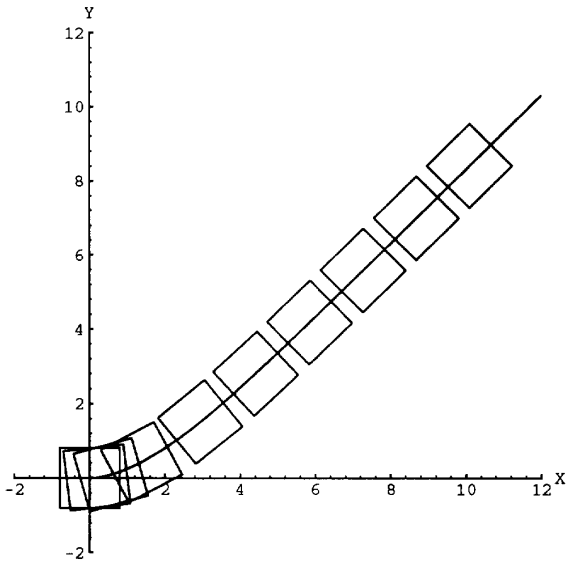

Fig. 6. Trajectory of the point P_o for Case ii).

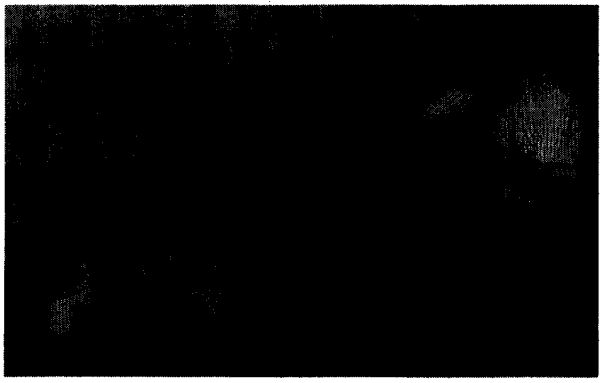

Fig. 7. Mobile manipulator used in three experiments.

the preferred configuration, denoting them by θ_{1r} and θ_{2r}. Then the coordinates of the reference point with respect to the platform frame $X_c - Y_c$ is given by

$$x_r^c = x_b^c + L_1 \cos\theta_{1r} + L_2 \cos\left(\theta_{1r} + \theta_{2r}\right) \tag{27}$$

$$y_r^c = y_b^c + L_1 \sin\theta_{1r} + L_2 \sin\left(\theta_{1r} + \theta_{2r}\right). \tag{28}$$

We emphasize that x_r^c and y_r^c are constant and will be used in the representation of the output equation (19). The manipulator is regarded as a passive device whose dynamics are neglected. It is assumed that a human operator drags the end effector of the manipulator. The position of the end effector is given as the desired trajectory for the reference point P_r. The manipulator will be kept in the preferred configuration provided that the reference point is able to follow the desired trajectory. Any tracking error of the reference point will leave the manipulator out of the preferred configuration, resulting in a drop of manipulability measure. To account for measurement and communication delay in the simulation, a fixed number of sampling periods later, the current position of the end effector is made available to the mobile platform. Five sampling periods of delay are introduced in the simulation described below.

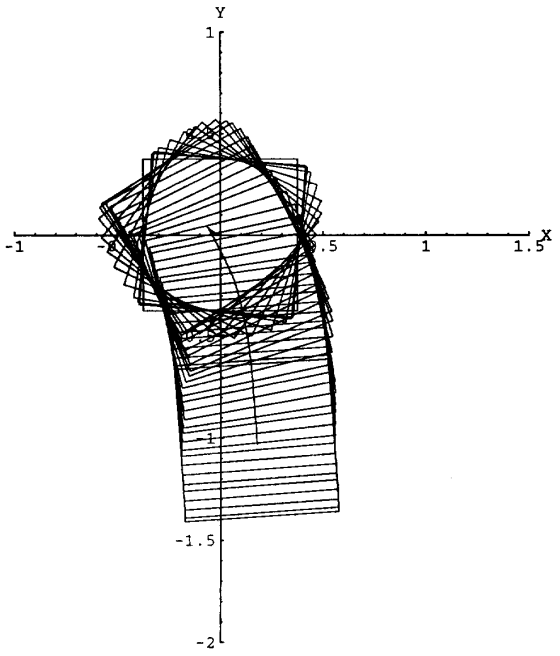

Fig. 8. Trajectory of the P_o and the motion of platform.

IV. Simulation

The mobile platform is initially directed toward positive X axis at rest and the initial configuration of the manipulator is $\theta_1 = -45°$ and $\theta_2 = 90°$. Two different paths used for the simulation are shown in Fig. 2. The velocity along the paths is constant.

1) *Case i)* Straight line perpendicular to the X axis or the initial forward direction of the mobile platform,
2) *Case ii)* Forward slanting line 45 degrees from X axis.

The sampling period is 0.01 sec. The linear state feedback gains for the two subsystems (22) and (23) are chosen so that the overall system has a natural frequency $w_n = 2.0$ and a damping ratio $\zeta = 1.2$. The higher damping ratio is to simulate the slow response of the mobile platform. For each simulation, we plot the trajectory of P_o, the trajectory of the reference point P_r, the manipulability measure, and the velocity of the P_o.

1) Fig. 3 shows the trajectory of point P_o, in which a box[2] represents the mobile platform. Note that the desired trajectory is given for the reference point P_r. P_o has no desired trajectory. We also note that the actual trajectory obtained for the reference point coincides with the given desired trajectory. The manipulability measure, and the velocity of point P_o are shown in Figs. 4 and 5, respectively. Fig. 4 shows a little degradation of manipulability measure corresponding to the early maneuver by the mobile platform. The negative value in Fig. 5 indicates that the mobile platform moved backward for a short period of time at the very beginning to achieve the needed heading angle. Note that the motion of the platform, or more precisely the trajectory of point P_o, is not planned. Therefore, the exhibited backward motion is not explicitly planned and is a consequence of the control algorithm. The presence of such backward motion depends on the direction of a desired trajectory, the desired velocity, and the location of the reference point.
2) The actual trajectory of the point P_o for the slanting trajectory is shown in Fig. 6. We omit the results for manipulability measure and the velocity of the point P_o due to their similarity to the Case i). The manipulability measure is kept near the optimal value with a small degradation in the beginning. A minor difference from the Case i) in terms of the velocity of P_o is that there is no backward motion observed in this case.

[2]These boxes are not equally distributed in time.

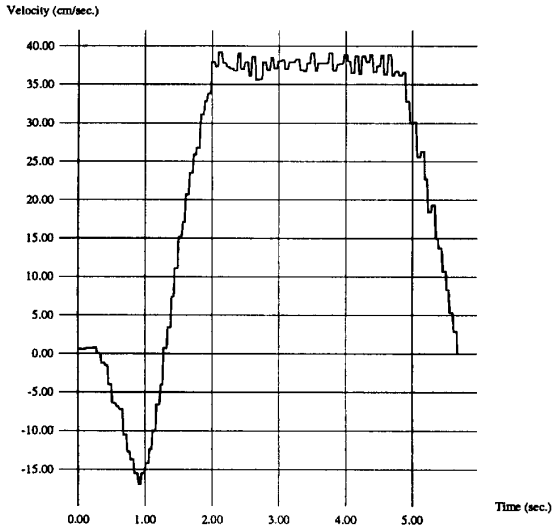

Fig. 9. Velocity of the point P_o of LABMATE®.

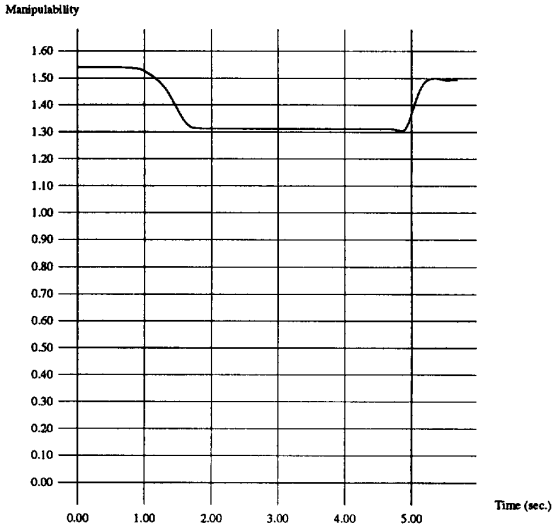

Fig. 10. Manipulability measure.

V. Experiment

The algorithm described above is implemented on an experimental mobile manipulator system. The system consists of a PUMA

250 6-DOF manipulator and a LABMATE® platform (Fig. 7). For simplicity only the first three joints of the manipulator are taken into account, i.e., no wrist joints are considered. The sampling rates of the PUMA 250 and the LABMATE® are 250 and 16 Hz, respectively. In the experiment, the end effector of the mobile manipulator which is at rest and in an optimal configuration in the beginning is dragged by a human operator. For comparison, it is dragged along the direction approximately normal to the initial heading direction of LABMATE®, which corresponds to the first trajectory in the simulations. Fig. 8 shows the trajectory of the point on the LABMATE® wheel axis (P_o). The trajectory indicates that the platform initially goes backward and then starts moving forward. This observation agrees with the simulation result. Fig. 9 depicts the velocity of the center of mass of the LABMATE®, which also indicates the presence of the initial backup. Note that dragging ceases at about six seconds. Manipulability measure is shown in Fig. 10. The manipulability drops slightly in the beginning and is maintained at the same level while the platform is in motion. It then comes back to a nearly optimal configuration after dragging ceases. The fact that the manipulability measure is kept near the maximum value implies that the reference point P_o closely follows the desired trajectory.

VI. Concluding Remarks

We presented a control algorithm for coordinating motion of a mobile manipulator. The design criterion was to control the mobile platform so that the manipulator is maintained at a configuration which maximizes the manipulability measure. The control algorithm is designed by using feedback linearization. Since the mobile platform is subject to nonholonomic constraints, the dynamic system governing the motion of the mobile platform is not input-state linearizable. Thus a nonlinear feedback is deployed to achieve input–output linearization. The output equations are chosen to be the coordinates of the end point of the manipulator when it is at the configuration with the maximum manipulability measure. The actual motion trajectory of the end point is used as the reference trajectory for the outputs of the mobile platform. We verified the effectiveness of our method by simulations on two representative trajectories. The algorithm was implemented with an actual mobile manipulator and the experimental results are consistent with those predicted by simulation. For future work, we will investigate the integration of the proposed method and force control. A path planning approach will be explored such that the maneuverability of mobile platform is taken into consideration as well.

References

[1] T. Yoshikawa, *Foundations of Robotics: Analysis and Control.* Cambridge, MA: MIT Press, 1990.

[2] J. Joshi and A. A. Desrochers, "Modeling and control of a mobile robot subject to disturbances," in *Proc. 1986 Int. Conf. Robotocs and Automation*, San Francisco, CA, Apr. 1986, pp. 1508–1513.

[3] G. J. Wiens, "Effects of dynamic coupling in mobile robotic systems," in *Proc. SME Robotics Research World Conf.*, Gaithersburg, MD, May 1989, pp. 43–57.

[4] K. Liu and F. L. Lewis, "Decentralized continuous robust controller for mobile robots," in *Proc. 1990 Int. Conf. Robotics and Automation*, Cincinnati, OH, May 1990, pp. 1822–1827.

[5] S. Dubowsky, P.-Y. Gu, and J. F. Deck, "The dynamic analysis of flexibility in mobile robotic manipulator systems, in *Proc. Eighth World Cong. Theory Machines and Mechanisms*, vol. 1, Prague, Czechoslovakia, August 1991, pp. 9–12.

[6] N. A. M. Hootsmans, "The motion control of manipulators on mobile vehicles," Ph.D. dissertation, Dept. Mech. Eng., MIT, Cambridge, MA, Jan. 1992.

[7] Ju. I. Neimark and N. A. Fufaev, *Dynamics of Nonholonomic Systems.* Providence, RI: American Mathematical Society, 1972.

[8] S. K. Saha and J. Angeles, "Dynamics of nonholonomic mechanical systems using a natural orthogonal complement," *ASME, J. Applied Mech.*, vol. 58, pp. 238–243, Mar. 1991.

[9] A. M. Bloch and N. H. McClamroch, "Control of mechanical systems with classical nonholonomic constraints," in *Proc. 28th IEEE Conf. Decision and Control*, Tampa, FL, Dec. 1989, pp. 201–205.

[10] A. M. Bloch, M. Reyhanoglu, and N. H. McClamroch, "Control and stabilization of nonholonomic dynamic systems," *IEEE Trans. Automat. Contr.*, vol. 37, no. 11, pp. 1746–1757, Nov. 1992.

[11] J. Barraquand and J.-C. Latombe, "On nonholonomic mobile robots and optimal maneuvering," in *Proc. Fourth IEEE Int. Symp. Intelligent Contr.*, Albany, NY, Sept. 1989, pp. 340–347.

[12] V. Kumar, X. Yun, E. Paljug, and N. Sarkar, "Control of contact conditions for manipulation with multiple robotic systems," in *Proc. 1991 Int. Conf. Robotics and Automation*, Sacramento, CA, Apr. 1991, pp. 170–175.

[13] A. M. Bloch, N. H. McClamroch, and M. Reyhanoglu, "Controllability and stabilizability properties of a nonholonomic control system," in *Proc. 29th IEEE Conf. Decision and Contr.*, Honolulu, HI, Dec. 1990, pp. 1312–1314.

[14] G. Campion, B. d'Andrea-Novel, and G. Bastin, "Controllability and state feedback stabilization of nonholonomic mechanical systems," in *Lecture Notes in Control and Information Science*, C. Canudas de Wit (Ed.). New York: Springer-Verlag, 1991, pp. 106–124.

[15] Y. Yamamoto and X. Yun, "Coordinating locomotion and manipulation of a mobile manipulator," in *Proc. 31st IEEE Conf. Decision and Contr.*, Tucson, AZ, Dec. 1992, pp. 2643–2648.

[16] J. P. Laumond, "Finding collision-free smooth trajectories for a nonholonomic mobile robot," in *10th Int. Joint Conf. Artificial Intelligence*, Milan, Italy, 1987, pp. 1120–1123.

[17] Z. Li and J. F. Canny, "Robot motion planning with nonholonomic constraints," Tech. Rep. UCB/ERL M89/13, Electronics Res. Lab., Univ. California, Berkeley, Feb. 1989.

[18] J.-C. Latombe, *Robot Motion Planning.* Boston: Kluwer, 1991.

[19] G. Lafferriere and H. Sussmann, "Motion planning for controllable systems without drift," in *Proc. 1991 Int. Conf. Robotics and Automation*, Sacramento, CA, Apr. 1991, pp. 1148–1153.

[20] B. d'Andrea-Novel, G. Bastin, and G. Campion, "Modeling and control of nonholonomic wheeled mobile robots," in *Proc. 1991 Int. Conf. Robotics and Automation*, Sacramento, CA, Apr. 1991, pp. 1130–1135.

[21] C. Samson and K. Ait-Abderrahim, "Feedback control of a nonholonomic wheeled cart in cartesian space," in *Proc. 1991 Int. Conf. Robotics and Automation*, Sacramento, CA, Apr. 1991, pp. 1136–1141.

[22] C. Canudas de Wit and R. Roskam, "Path following of a 2-DOF wheeled mobile robot under path and input torque constraints," in *Proc. 1991 Int. Conf. on Robotics and Automation*, Sacramento, CA, Apr. 1991, pp. 1142–1147.

[23] H. Nijmeijer and A. J. van der Schaft, *Nonlinear Dynamic Control Systems.* New York: Springer-Verlag, 1990.